Ground-state geometries and optical properties of $Na_{8-x}Li_x$ $(x=0-8)$ clusters

M. D. Deshpande,* D. G. Kanhere,† and P. V. Panat
Department of Physics, University of Pune, Pune 411007, India

Igor Vasiliev‡ and Richard M. Martin§
Department of Physics, University of Illinois at Urbana-Champaign, Urbana, Illinois 61801

(Received 5 December 2001; published 3 May 2002)

We have investigated equilibrium geometries of mixed clusters $Na_{8-x}Li_x$ $(x=0-8)$ using *ab initio* molecular dynamics within the framework of density functional theory. The resulting cluster geometries show evolution from C_{3v} symmetry for Li_8 to D_{2d} symmetry for Na_8 via T_d symmetry (Li_4Na_4). We also present and discuss the absorption spectra obtained using the time-dependent local density approximation formalism. The calculated absorption spectra of all $Na_{8-x}Li_x$ clusters demonstrate the presence of a strong plasmon peak located approximately at the same energy (≈ 2.7 eV). Our calculations predict nearly the same oscillator strengths for the main plasmon peaks of Li_8 and Na_8. Since the polarizabilities of Li_8 (9.7 Å^3) and Na_8 (14.02 Å^3) are significantly different, the above observation indicates the significance of nonplasmon contributions in the optical spectrum of Li_8 and implies that the simple jellium approach and the plasmon pole approximation are not valid for Li_8.

DOI: 10.1103/PhysRevA.65.053204 PACS number(s): 36.40.Qv, 36.40.Mr, 61.46.+w, 31.15.Ar

I. INTRODUCTION

Over the last two decades, alkali-metal clusters have been extensively studied both experimentally and theoretically. Many of these studies have concentrated on the size dependence of geometries, energetics, and structural stability. One of the interesting features discovered in such studies was the existences of ''magic'' clusters that have exceptional stability. While a number of basic characteristics of these clusters can be derived from a spherical jellium model [1,2], more sophisticated theoretical methods are required to obtain the structural details which are essential for understanding many physical and electronic properties such as vibrational frequencies, ionization potentials, polarizabilities, and absorption spectra. Despite a large number of studies carried out for small homogeneous alkali clusters, only a few reports are available for mixed alkali-metal clusters [3–7]. Studies of absorption spectra and polarizabilities of alkali-metal clusters are of particular interest since the polarizability and the shape of the optical spectrum depend upon the structure and size of the cluster. Recently, measurements of the total photoabsorption cross section of alkali-metal clusters were fitted to a collective resonance model, which used the principal values of the static polarizability tensor as fit parameters. The structure and characteristics of the resonant peaks observed in absorption spectra should, therefore, reflect the deviations of the true cluster geometry from the ''perfect'' spherical shape. Available studies of mixed sodium-lithium clusters [8–15] show that the topology of alkali-metal clusters varies with the composition and that the excited-state properties of such clusters are modified with the change of Li/Na content. Motivated by these observations, we have performed a systematic study of mixed clusters $Na_{8-x}Li_x$ $(x=0-8)$ using *ab initio* molecular dynamics within the framework of density functional theory (DFT). We have also calculate polarizabilities using a finite-field method [16] and absorption spectra using a real-space time-dependent local density approximation (TDLDA) formalism [17]. It is interesting to note that all the studied systems are eight-electron systems with completely filled sp shells that represent ''magic'' clusters. Therefore, systematic evolution of properties like geometries, energetics, and optical properties will reflect the details of the electronic structure beyond the jellium model.

In Sec. II we briefly discuss the computational methods and numerical details; the results of our calculations and their discussion are presented in Sec. III.

II. COMPUTATIONAL DETAILS

Our calculations have been carried out in two steps. In the first step, we performed *ab initio* Born-Oppenheimer molecular dynamics simulations to obtain the equilibrium geometries. We used an efficient scheme based on the damped second-order equation of motion and the integration scheme proposed by Payne *et al.* [18]. This technique permitted us to use a fairly large time step of ≈ 100 a.u. All the cluster geometries were obtained by starting with an unbiased configuration, which was heated up to 600–800 K, followed by slow cooling. We used the norm conserving nonlocal pseudopotentials of Bachelet, Hamann, and Schluter [19] with the p component taken as local and the Barth-Hedin exchange-correlation potential [20]. In our calculations we used a periodic cell of 40 a.u. and an energy cutoff of approximately 11 Ry. In all cases, the stability of the ground-state configuration was tested by reheating the cluster and allowing it to span the configuration space, and then cooling it down to get the lowest-energy configuration. In the second step, these geometries were refined with a real-space code [17,21] using the generalized gradient approximation (GGA) of Perdew *et al.* [22] for the exchange-correlation term. The refined

*Email address: mdd@physics.unipune.ernet.in
†Email address: kanhere@physics.unipune.ernet.in
‡Email address: vasiliev@uiuc.edu
§Email address: rmartin@uiuc.edu

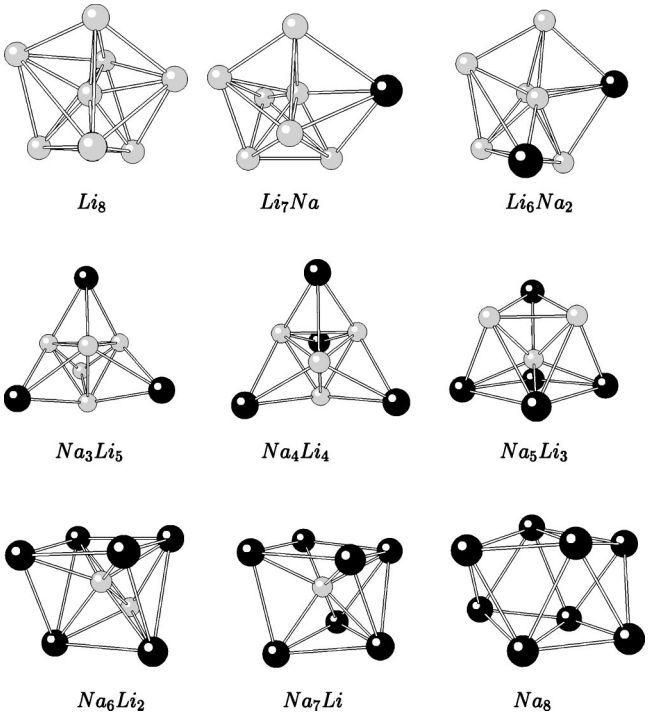

FIG. 1. Equilibrium geometries of $Na_{8-x}Li_x$ $(x=0-8)$ clusters. The dark and light circles represent Na and Li atoms, respectively.

ground-state geometries are identical in symmetry with that of the local-density approximation (LDA) geometries and their bond lengths differ by not more than 4%. It is known that use of the GGA improves the polarizabilities, bringing them near to the experimental results [6]. The optical spectrum via the TDLDA was calculated using the LDA exchange-correlation potential [23]. The exchange-correlation term was approximated with the Ceperley-Alder exchange-correlation functional [24]. In these calculations, we used a grid spacing of $h=0.4$ a.u. The grid was set up inside a spherical boundary with a radius of 15 a.u. These calculations were based on the Troullier-Martins nonlocal pseudopotentials [25]. Polarizabilities were calculated using a finite-field approach [16] with a grid spacing of $h=0.6$ a.u., radius of the spherical boundary of 22 a.u., and an applied external electric field of 10^{-3} a.u. A somewhat larger grid spacing of 0.8 a.u. and sphere of radius 25 a.u. were used for the calculation of the spectrum. Inclusion of about 60 excited states was found to be sufficient to obtained well converged spectra.

III. RESULTS AND DISCUSSION

Equilibrium geometries of $Na_{8-x}Li_x$ $(x=0-8)$ clusters are shown in Fig. 1. We note that the binding energies of the diatomic systems Na-Li, Na-Na, and Li-Li are 0.76 eV, 0.71 eV, and 0.79 eV, respectively, which indicate that the Li-Li bond is the strongest and the Na-Li bond is slightly stronger than the Na-Na bond. In our earlier studies [6], we observed a tendency for a single Na atom to be on the surface of Li clusters. We attributed this tendency to the weaker binding of Na with Li (as compared to Li-Li) and to the larger ionic

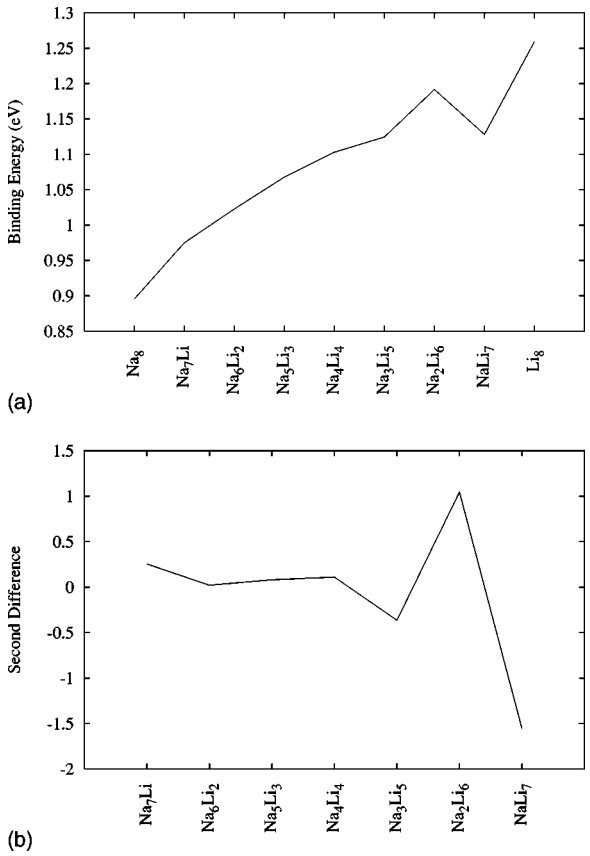

FIG. 2. (a) Binding energies per atom and (b) second differences in energy for $Na_{8-x}Li_x$ $(x=0-8)$ clusters shown as a function of the total number of atoms.

radius of Na (1.80 a.u.) than that of Li (1.13 a.u.).

In good agreement with other available calculations [26,27], we find that the lowest-energy structure of Li_8 is a centered trigonal prism with an atom capping one of the rectangular faces, which has the C_{3v} symmetry, and the structure of Na_8 is a dodecahedron with the D_{2d} symmetry. The geometries of $Na_{8-x}Li_x$ $(x=0-8)$ clusters can be grouped according to their symmetry as follows: (1) C_{3v} (Li_8, Li_7Na Li_6Na_2), (2) T_d (Li_5Na_3, Li_4Na_4, Li_3Na_5), and (3) D_{2d} (Li_2Na_6, $LiNa_7$, Na_8). In other words, as the sodium content increases across the series, the transition from the C_{3v} to D_{2d} structures occurs via the T_d (Li_4Na_4) symmetry. The lowest-energy structure for Li_7Na is similar to that of Li_8. As expected, the Na impurity in Li_8 remains on the surface accompanied by a slight distortion of the cluster structure. The second Na atom in Li_6Na_2 substitutes for one of the Li atoms in such a way that it avoids bond formation with the other Na atom and simultaneously maximizes the number of Na-Li bonds. The trend to replace the surface Li atoms continues with the addition of more Na atoms. This is also accompanied by the change in the overall cluster symmetry. The shape of the next cluster, Li_5Na_3, resembles a stellated tetrahedron (T_d). The addition of the fourth Na atom produces a tetracapped tetrahedron structure (T_d), where the four Li atoms form the inner tetrahedron and the remaining Na atoms form the capping structure. The Na-dominated clusters Na_6Li_2 and $LiNa_7$ show a tendency to-

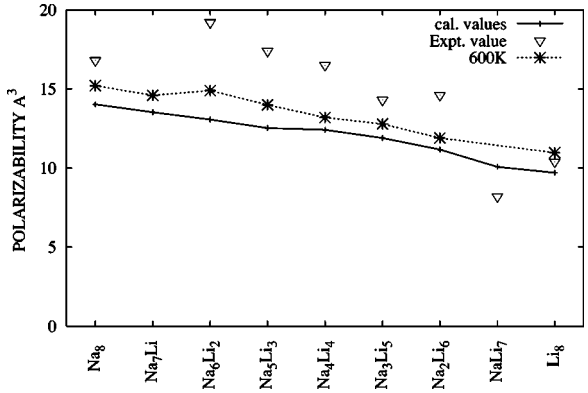

FIG. 3. Polarizabilities of $Na_{8-x}Li_x$ ($x=0-8$) clusters. Triangles, experimental data [13]; solid line, theory at $T=0$ K; stars (dotted line), theory at $T=600$ K.

ward the D_{2d} symmetry rather than T_d. In the case of Na_6Li_2, the two Li atoms take a position in the core of the cluster, which can be explained by the stronger Li-Li bond. In the case of Na_7Li, the single Li impurity is trapped almost near the center of the cluster and the overall structure resembles a distorted dodecahedron (D_{2d}).

We now discuss the stability of these clusters based on binding energies per atom E_b and second differences Δ^2E shown in Figs. 2(a) and 2(b). The binding energy per atom and the second difference are defined as

$$E_b[Na_xLi_{8-x}]=\{-E[Na_xLi_{8-x}]+xE[Na]+(8-x)E[Li]\}/8, \quad (1)$$

$$\Delta^2E[Na_xLi_{8-x}]=-2E[Na_xLi_{8-x}]+E[Na_{x+1}Li]+E[Na_{x-1}Li]. \quad (2)$$

In general, the binding energies of clusters increase from Na_8 to Li_8. However, the binding energy for Li_7Na shows a sharp dip, which correlates quite well with a reduction in the highest occupied molecular orbital–lowest unoccupied molecular orbital (HOMO-LUMO) gap for this cluster (not shown). The substitution of two Li atoms by Na atoms makes the Li_6Na_2 cluster nearly spherical, and enhances its binding energy by 0.06 eV as compared to Li_7Na. Since the maximum in the second difference signifies enhanced stability, Li_6Na_2 turns out to be the most stable structure in the series. The evolution of the symmetry of these clusters across the series is reflected in their optical spectra and will be discussed below.

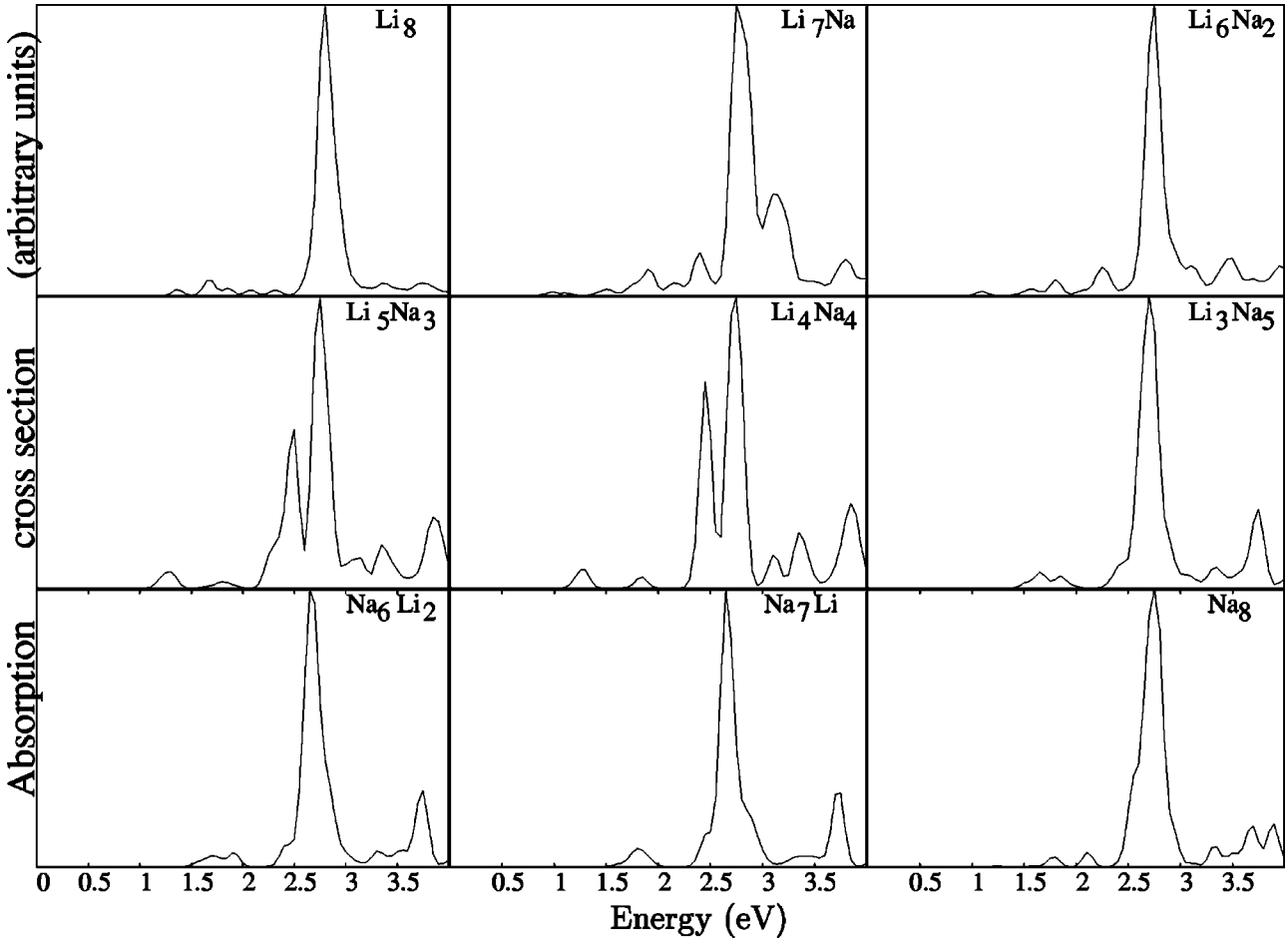

FIG. 4. Calculated TDLDA absorption spectra of $Na_{8-x}Li_x$ clusters. All spectra are broadened by 0.06 eV to simulate finite temperature.

The calculated polarizabilities per atom for $Na_{8-x}Li_x$ ($x=0-8$) clusters are shown in Fig. 3 along with the available experimental values [13]. It may be noted that the atomic polarizabilities of Li (23.6 A^3) and Na (24.8 A^3) are close to each other. However, the polarizability of the Na_8 cluster is significantly higher than that of Li_8. For the most part, polarizabilities decrease continuously with increasing fraction of Li atoms in the clusters. As expected, the experimental polarizability values are considerably underestimated by the zero-temperature calculations. It has been shown [28,29] that the discrepancy between theory and experiment can be significantly reduced by incorporating finite-temperature effects. To improve agreement with experiment, we have also computed cluster polarizabilities at 600 K using molecular dynamics simulations and calculating polarizabilities at several random sampling points. The resulting average polarizabilities are shown in Fig. 3 (dotted line). Our calculations show that including the finite-temperature effects reduces the average error between theory and experiment from approximately 21% to 13%.

In Fig. 4, we present absorption spectra of $Na_{8-x}Li_x$ ($x=0-8$) clusters. These spectra exhibit several interesting features. All calculated spectra demonstrate the presence of a strong plasmon peak. This peak is positioned approximately at the same energy throughout the series (≈ 2.7 eV). The substitution of one Li atom with Na introduces an extra shoulder on the high-energy side of the absorption spectrum. For clusters in the middle of the series, such as Li_5Na_3 and Li_4Na_4, an extra peak is developed on the lower-energy side of the spectrum. These features are closely related to the evolution of the charge density across the series. The total density isosurfaces for Li_8, Li_7Na, Li_4Na_4, and Na_8 are shown in Fig. 5. The charge density distribution is nearly spherically symmetric for Na_8 and Li_8. This distribution becomes spheroidal with the substitution of a single Na atom for Li_8 (Li_7Na). For Na_4Li_4, the charge density distribution is nonspherical and possesses the T_d symmetry. As a rule, the oscillator strength in absorption spectra of clusters with a nonspherical charge distribution is spread over a wide energy range, thus leading to broader overall spectra.

The single peak for Na_8 and Li_8 is consistent with the nearly spherical shape of these clusters [26,30]. The splitting of the plasmon line for some of the clusters studied might be related to the deviations of the overall cluster shape from spherical symmetry. Within the jellium model, such splitting could be explained by allowing for ellipsoidal or more complex deformations of the cluster shape [31,32]. According to our earlier discussion, the overall cluster symmetry changes from C_{3v} for Li_8 to D_{2d} for Na_8. This transition occurs via the T_d symmetry. For clusters with T_d symmetry, such as Li_5Na_3 and Li_4Na_4, we observe a splitting of the main plasmon line. The spectra of these clusters clearly show two separate peaks, one having approximately twice the strength of the other.

The mean static polarizability α is related to the absorption properties through the perturbation theory expression [29,33–35]

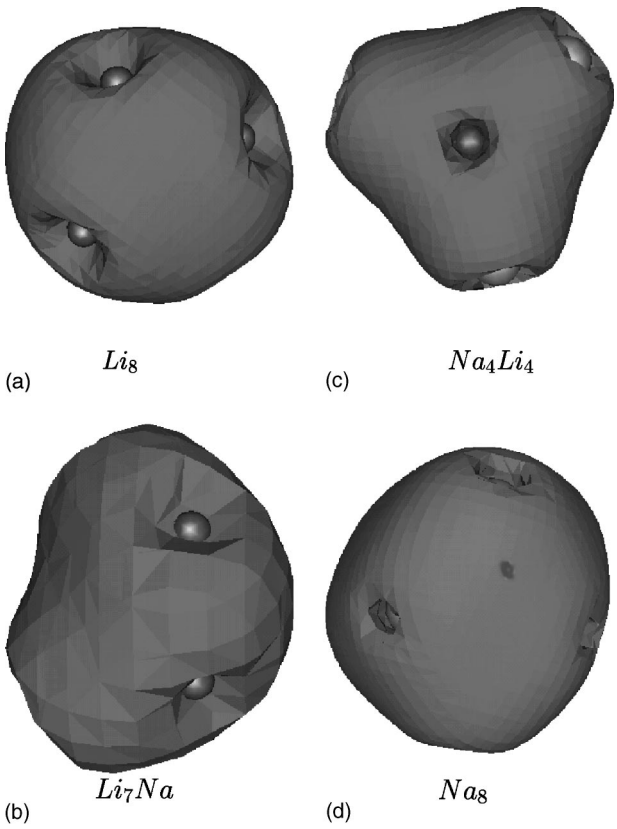

FIG. 5. Spatial distribution of the valence charge density (core density excluded) for (a) Li_8, (b) Li_7Na, (c) Li_4Na_4, and (d) Na_8.

$$\alpha = \sum_i F_n/\Omega_n^2, \tag{3}$$

where F_n is the oscillator strength and Ω_n is the transition energy. Under the plasmon pole approximation, this expression can be reduced to

$$\alpha = F_p/\Omega_p^2, \tag{4}$$

where Ω_p refers to the plasmon energy. The plasmon pole approximation has been shown to yield a reasonable value for the polarizability of Na_8 (25 a.u.) [36]. According to this approximation, the polarizability increases with increasing oscillator strength and decreases with increasing plasmon energy. Since the plasmon energy is roughly the same for both Li_8 and Na_8 clusters, the difference in their polarizabilities within the plasmon pole approximation can only be explained by the difference in the oscillator strengths of the plasmon peak. However, our TDLDA calculations predict nearly the same oscillator strengths for the main plasmon peaks of Li_8 and Na_8. Consequently, the difference in polarizabilities of Li_8 and Na_8 indicate that the nonplasmon contributions are significant. Thus, the simple jellium approach and the plasmon pole approximation are no longer accurate in the case of Li_8.

IV. CONCLUSIONS

We have calculated the equilibrium geometries of mixed clusters $Na_{8-x}Li_x$ ($x=0-8$) using *ab initio* molecular dy-

namics within the framework of density functional theory. As the sodium content increases across the series, the transition from C_{3v} to D_{2d} symmetry occurs via T_d (Li_4Na_4) symmetry. We have also calculated polarizabilities and optical absorption spectra of these clusters. The calculated absorption spectra of all $Na_{8-x}Li_x$ clusters demonstrate the presence of a strong plasmon peak throughout the series. The single peak for Na_8 and Li_8 is consistent with the nearly spherical shape of these clusters. For nonspherical clusters, such as Li_4Na_4, the oscillator strength is distributed over a wide energy range leading to a broader overall spectrum. The difference in polarizabilities of Li_8 and Na_8 indicates significant nonplasmon contributions in the optical spectrum of Li_8, which suggests that the plasmon pole approximation is no longer valid in the case of Li_8.

ACKNOWLEDGMENTS

We gratefully acknowledge the Indo-French Center for the Promotion of Advanced Research (New Delhi) (Centre Franco-Indian Pour la Promotion de la Recherche Avancée). M.D. acknowledges the University Grants Commission, India for financial support. I.V. and R.M.M. acknowledge support for this work by the National Science Foundation under Grant No. DMR 99-76550 for the Materials Computation Center at the University of Illinois and Grant No. DMR 98-02373.

[1] W.D. Knight, K. Clemenger, W.A. de Heer, W.A. Saunders, M.Y. Chou, and M.L. Cohen, Phys. Rev. Lett. **52**, 2141 (1984).
[2] M.Y. Chou and M.L. Cohen, Phys. Lett. **113A**, 420 (1986).
[3] Yasuhiro Senda, Fuyuki Shimojo, and Kazo Hoshino, J. Phys. Soc. Jpn. **67**, 916 (1998).
[4] M.J. Lopez, M.P. Iniguez, and J.A. Alonso, Phys. Rev. B **41**, 5636 (1990).
[5] M.M. Kappes, M. Schar, and E. Schumacher, J. Phys. Chem. **91**, 658 (1987).
[6] M.D. Deshpande, D.G. Kanhere, Igor Vasiliev, and Richard M. Martin, Phys. Rev. A **65**, 033202 (2002).
[7] E. Benichou, A.R. Allouche, M. Aubert-Frecon, R. Antonie, M. Broyer, Ph. Dugourd, and D. Rayane, Chem. Phys. Lett. **290**, 171 (1998).
[8] T.A. Dahlseid, Manfred M. Kappes, John A. Pople, and Mark A. Ratner, J. Chem. Phys. **96**, 4924 (1992).
[9] Stuart Pollack, C.R.C. Wang, Tina A. Dahlseid, and Manfred M. Kappes, J. Chem. Phys. **96**, 4918 (1992).
[10] V. Bonačić-Koutecký, P. Fantucci, J. Gaus, and J. Koutecký, Z. Phys. D: At., Mol. Clusters **19**, 37 (1991); V. Bonačić-Koutecký, J. Gaus, M.F. Guest, and J. Koutecky̆, J. Chem. Phys. **96**, 4934 (1992).
[11] Y. Saito and T. Noda, Z. Phys. D: At., Mol. Clusters **19**, 129 (1991).
[12] W.D. Knight, Keith Clemenger, Walt A. de Heer, and Winston A. Saunders, Phys. Rev. B **31**, 2539 (1985).
[13] R. Antoine, D. Rayane, A.R. Allouche, M. Aubert-Frecon, E. Benichou, F.W. Dalby, Ph. Dugourd, M. Broyer, and C. Guet, J. Chem. Phys. **110**, 5568 (1999).
[14] D. Rayane, A.R. Allouche, E. Benichou, R. Antine, M. Aubert-Frecon, Ph. Dugourd, M. Broyer, C. Ristori, F. Chandezon, B.A. Huber, and C. Guet, Eur. Phys. J. D **9**, 243 (1999).
[15] I. Moullet, Jose Luis Martins, F. Reuse, and Jean Buttet, Phys. Rev. Lett. **65**, 476 (1990).
[16] Igor Vasiliev, Serdar Ogut, and James R. Chelikowsky, Phys. Rev. Lett. **78**, 4805 (1997).
[17] Igor Vasiliev, Serdar Ogut, and James R. Chelikowsky, Phys. Rev. Lett. **82**, 1919 (1999), and references therein.
[18] M.C. Payne, J.D. Joannopoulos, D.C. Allan, M.P. Teter, and D.H. Vanderbilt, Phys. Rev. Lett. **56**, 2656 (1986); M.C. Payne, M.P. Teter, D.C. Allan, T.A. Arias, and J.D. Joannopoulos, Rev. Mod. Phys. **64**, 1045 (1992).
[19] G.B. Bachelet, D.R. Hamann, and M. Schluter, Phys. Rev. B **26**, 4199 (1982).
[20] U. Barth and L. Hedin, J. Phys. C **5**, 1269 (1972).
[21] J.R. Chelikowsky, N. Troullier, and Y. Saad, Phys. Rev. Lett. **72**, 1240 (1994); J.R. Chelikowsky, N. Troullier, K. Wu, and Y. Saad, Phys. Rev. B **50**, 11 355 (1994).
[22] J.P. Perdew, J.A. Chevary, S.H. Vosko, K.A. Jackson, M.R. Pederson, D.J. Singh, and C. Fiolhais, Phys. Rev. B **46**, 6671 (1992); **48**, 4978 (1993).
[23] The present version of the TDLDA code is not implemented for GGA and hence we are constrained to use the LDA approximation for exchange correlation for the optical spectrum.
[24] D.M. Ceperley and B.J. Alder, Phys. Rev. Lett. **45**, 566 (1980); J.P. Perdew and A. Zunger, Phys. Rev. B **23**, 5048 (1981); D.E. Beck, *ibid.* **43**, 7301 (1991).
[25] N. Troullier and J.L. Martins, Phys. Rev. B **43**, 1993 (1991).
[26] Angel Rubio, J.A. Alonso, X. Blase, L.C. Balbas, and Steven G. Louie, Phys. Rev. Lett. **77**, 247 (1996).
[27] U. Rothlisberger and W. Andreoni, J. Chem. Phys. **94**, 8129 (1991).
[28] Leeor Kronik, Igor Vasiliev, Manish Jain, and James R. Chelikowsky, J. Chem. Phys. **115**, 4322 (2001).
[29] Leeor Kronik, Igor Vasiliev, and James R. Chelikowsky, Phys. Rev. B **62**, 9992 (2000).
[30] J.M. Pacheco and Jose Luis Martins, J. Chem. Phys. **106**, 6039 (1997); J.M. Pacheco and W.D. Schone, Phys. Rev. Lett. **79**, 4986 (1997).
[31] Keith Clemenger, Phys. Rev. B **32**, 1359 (1985).
[32] J. Blanc, V. Bonačić-Koutecký, M. Broyer, J. Chevaleyre, Ph. Dugourd, J. Koutecký, C. Scheuch, J.P. Wolf, and L. Woste, J. Chem. Phys. **96**, 1793 (1992).
[33] C.R. Chris Wang, Stuart Pollack, Douglas Cameron, and Manfred M. Kappes, J. Chem. Phys. **93**, 3787 (1990).
[34] Kathy Selby, Vitaly Kresin, Jun Masui, Michael Vollmer, Walt A. de Heer, Adi Scheidemann, and W.D. Knight, Phys. Rev. B **43**, 4565 (1991).
[35] Kathy Selby, Michael Vollmer, Jun Masui, Vitaly Kresin, Walt A. de Heer, and W.D. Knight, Phys. Rev. B **40**, 5417 (1989).
[36] Z. Penzar, W. Ekardt, and A. Rubio, Phys. Rev. B **42**, 5040 (1990).